

## Extended spectral response in organic photomultiple photodetectors using multiple near-infrared dopants

Shao-Tang Chuang, Shang-Chieh Chien, and Fang-Chung Chen

Citation: *Applied Physics Letters* **100**, 013309 (2012); doi: 10.1063/1.3675573

View online: <http://dx.doi.org/10.1063/1.3675573>

View Table of Contents: <http://scitation.aip.org/content/aip/journal/apl/100/1?ver=pdfcov>

Published by the *AIP Publishing*

---

### Articles you may be interested in

Temperature dependent dielectric function in the near-infrared to vacuum-ultraviolet ultraviolet spectral range of alumina and yttria stabilized zirconia thin films

*J. Appl. Phys.* **114**, 223509 (2013); 10.1063/1.4844515

High quantum efficiency InGaN/GaN multiple quantum well solar cells with spectral response extending out to 520 nm

*Appl. Phys. Lett.* **98**, 201107 (2011); 10.1063/1.3591976

Highly sensitive, low-voltage, organic photomultiple photodetectors exhibiting broadband response

*Appl. Phys. Lett.* **97**, 103301 (2010); 10.1063/1.3488017

Spectral function and responsivity of resonant tunneling and superlattice quantum dot infrared photodetectors using Green's function

*J. Appl. Phys.* **102**, 083108 (2007); 10.1063/1.2799075

Near-infrared photoconductive and photovoltaic devices using single-wall carbon nanotubes in conductive polymer films

*J. Appl. Phys.* **98**, 084314 (2005); 10.1063/1.2113419

---

The advertisement features a dark blue background with white and orange text. At the top left, it reads 'NEW! Asylum Research MFP-3D Infinity™ AFM' in large white letters, with 'Unmatched Performance, Versatility and Support' in orange below it. The Oxford Instruments logo is in the top right corner, with the tagline 'The Business of Science®' underneath. The central area contains four key benefits, each with a small image: 'Stunning high performance' (micrograph), 'Simpler than ever to GetStarted™' (micrograph), 'Comprehensive tools for nanomechanics' (micrograph), and 'Widest range of accessories for materials science and bioscience' (micrograph). On the right, a photograph of the MFP-3D Infinity AFM instrument is shown.

## Extended spectral response in organic photomultiple photodetectors using multiple near-infrared dopants

Shao-Tang Chuang,<sup>1,2</sup> Shang-Chieh Chien,<sup>1,3</sup> and Fang-Chung Chen<sup>1,2,a)</sup>

<sup>1</sup>Department of Photonics, National Chiao Tung University, Hsinchu 30010, Taiwan

<sup>2</sup>Display Institute, National Chiao Tung University, Hsinchu 30010, Taiwan

<sup>3</sup>Institute of Electro-Optical Engineering, National Chiao Tung University, Hsinchu 30013, Taiwan

(Received 2 December 2011; accepted 15 December 2011; published online 6 January 2012)

We demonstrate highly sensitive polymer photodetectors (OPDs) with spectral response extending from the ultraviolet to the near-infrared (NIR) region ( $\sim 1200$  nm). After doping two NIR dopants, high external quantum efficiencies ( $\sim 5500\%$ ) and high responsivities ( $23.0$  A/W) are achieved under a low reverse bias ( $-3.7$  V). The high gains could be attributed to unbalanced carrier transport in the photoactive layer arising from the electron traps at the NIR dopants. This approach allows the ready preparation of OPDs exhibiting broad spectral responses and high quantum efficiencies simultaneously. © 2012 American Institute of Physics. [doi:10.1063/1.3675573]

Organic photodetectors (OPDs) are receiving enormous attention due to their advantageous properties of low cost, light weight, and flexibility.<sup>1–7</sup> Many potential applications, such as flexible sheet image scanners<sup>4</sup> and hemispherical focal plane detector arrays which can function as human eyes,<sup>5</sup> have been proposed for flexible OPDs. More recently, OPDs with broad spectral response have become the research focus. Because the sensing range of these devices can be extended into the near-infrared (NIR) wavelength ( $\lambda$ ) range, the OPDs would have many additional potential applications in such fields as night vision surveillance, remote controls, and optical communication.<sup>1,2</sup> However, the quantum efficiencies of the OPDs were still relatively lower than those of the inorganic counterparts, especially in the long wavelength range.

Photomultiplication (PM), a phenomenon in which the quantum efficiency of charge generation exceeds 100%, in organic photodiodes was reported in 1994.<sup>8</sup> Subsequently, many highly efficient OPDs based on the PM phenomenon have been demonstrated.<sup>9–15</sup> For example, Chen *et al.* blended CdTe nanoparticles into polymer photodiodes and achieved a high external quantum efficiency (EQE) of  $\sim 8000\%$  under conditions of low reverse bias.<sup>9</sup> They attributed the PM phenomenon to photogenerated electron trapping which assists hole injection into the device. Recently, we have also demonstrated highly sensitive organic PM photodetectors exhibiting broadband response ranging from ultraviolet (UV) to NIR spectral region.<sup>10</sup> After doping an organic NIR dye into the active layer of the photodiode, high EQEs could be obtained. Herein, we demonstrate organic PM photodetectors which can further extend the spectral response range to  $\sim 1200$  nm through codoping of two NIR dyes into the photoactive layer.

The conjugated polymer and fullerene derivative used in this study were regioregular poly(3-hexylthiophene) (P3HT) and 1-(3-methoxycarbonyl)propyl-1-phenyl[6,6]methanofullerene (PCBM), respectively. The NIR dopants were Ir-125 and Q-Switch 1, which were purchased from Exciton Corp.

and were used as received. The chemical structures of the materials used are displayed in Fig. 1(a). Figure 1(b) shows that the optical absorption of the P3HT:PCBM thin films in the NIR regime increased after doping of Ir-125 and Q-Switch 1 molecules. For the device fabrication, poly(3,4-ethylenedioxythiophene):poly(styrene sulfonate) (PEDOT:PSS) was spin-coated onto the indium tin oxide (ITO)-coated substrates and the resulting film was baked at  $120^\circ\text{C}$  for 1 h. Then, P3HT/PCBM blends dissolved in 1,2-dichlorobenzene were further coated onto top of the PEDOT:PSS layer.

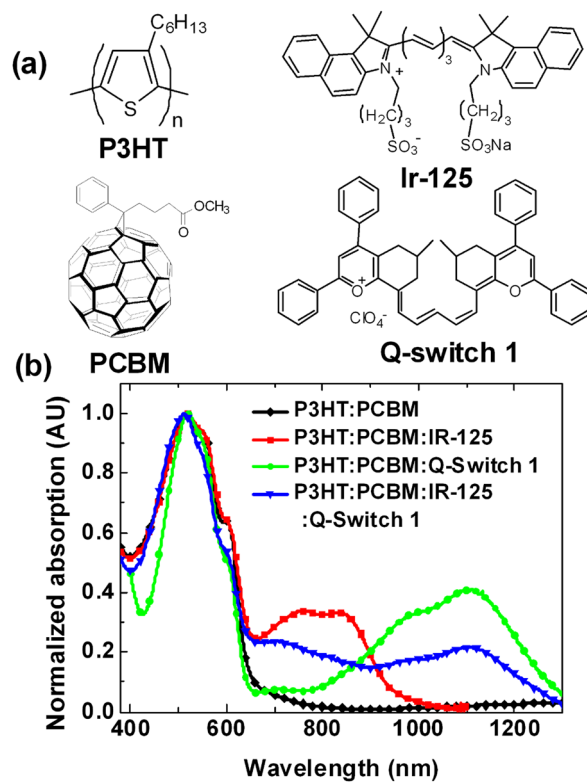


FIG. 1. (Color online) (a) Chemical structures of P3HT, PCBM, Ir-125 and Q-switch 1. (b) Absorption spectra of the P3HT:PCBM film, the P3HT:PCBM film containing Ir-125 [P3HT:PCBM:Ir-125, 1:1:1 (w/w/w)], the P3HT:PCBM film containing Q-switch 1 [P3HT:PCBM:Q-switch 1, 1:1:1 (w/w/w)], and the P3HT:PCBM film containing both Ir-125 and Q-switch 1 [P3HT:PCBM:Ir-125:Q-switch 1, 1:1:0.5:0.5 (w/w/w)].

<sup>a)</sup>Author to whom correspondence should be addressed. Electronic mail: fcchen@mail.nctu.edu.tw.

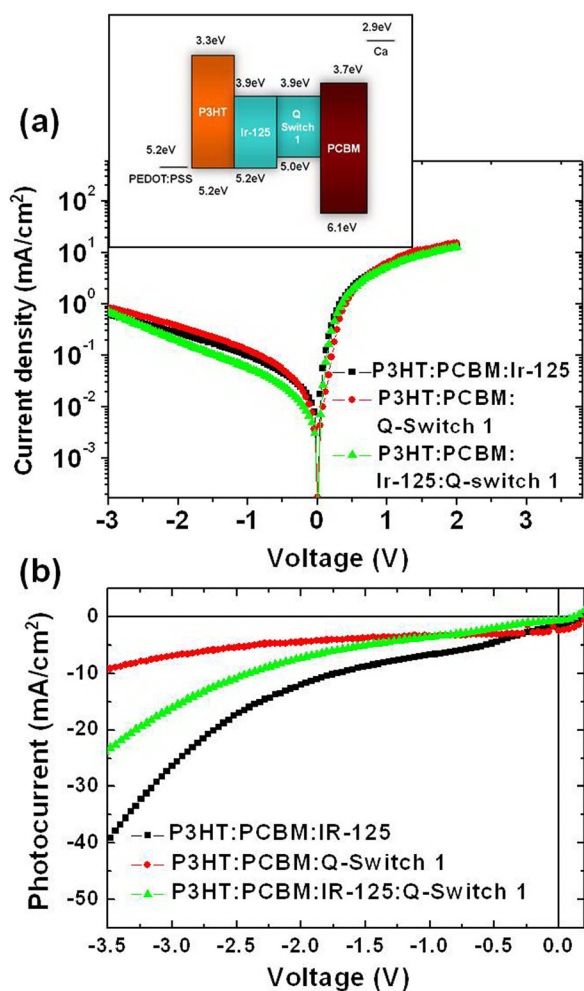


FIG. 2. (Color online) (a) Log-scale current density-voltage curves of the devices measured in the dark. Inset: energy level diagram for the materials used in this study. (b)  $J$ - $V$  curves of the devices prepared with various NIR dyes under illumination (simulated AM1.5G). A neutral density filter was used to reduce the light intensity down to  $33.3 \text{ mW cm}^{-2}$ .

To fabricate PM OPDs, Ir-125 and/or Q-Switch 1 molecules were further doped into the polymer blend. Finally, the metals Ca (50 nm) and Al (100 nm) were thermally evaporated to form the bilayer cathode. For the device characteristics, the photocurrent density-voltage ( $J$ - $V$ ) curves under illumination were measured using the Keithley 2400 measurement system. The light source was a Thermal Oriel solar simulator, whose illumination intensity was calibrated using a standard Si photodiode detector equipped with a KG-5 filter (Hamamatsu, Inc.).<sup>16</sup> For the EQE measurements, the incident light passing through a monochromator (SpectraPro-2510i, Action Research Corp.) was chopped at 100 Hz. The resulting photocurrent was measured by using the lock-in amplifier (SR570, Stanford Research Corp.).

Figure 2(a) provides current-voltage curves of the devices containing various dopants measured in the dark. Clear diode characteristics, with current rectification ratios of ca.  $10^2$  at  $\pm 2 \text{ V}$  bias for all the devices, could be observed. Figure 2(b) shows the  $J$ - $V$  curves for the devices doped with either Ir-125, Q-Switch 1 or both dyes. Apparently, for all the three types of devices, we could observe large photocurrent, suggesting that high photoconductive gains were obtained. To understand the origins of high level of photocurrent den-

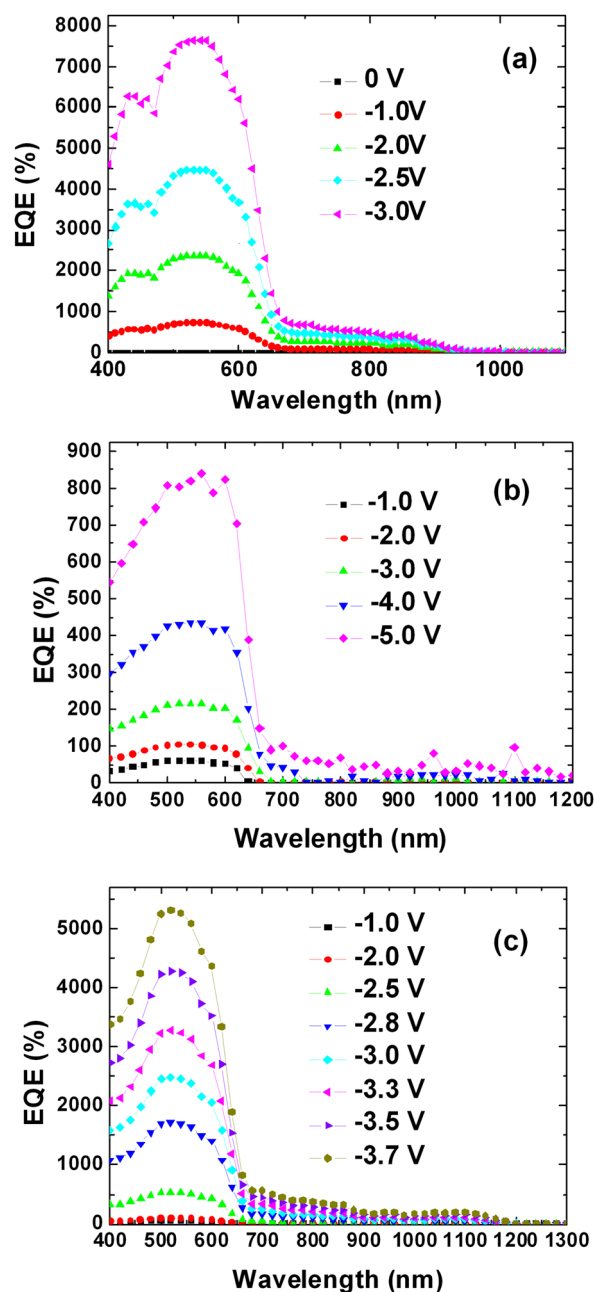


FIG. 3. (Color online) EQE spectra of the devices prepared with various NIR dyes under different reverse bias conditions. Device structure: ITO/PEDOT:PSS/P3HT:PCBM:NIR molecules/Ca/Al. Material weight ratios: (a) P3HT:PCBM:Ir-125 = 1:1:1, (b) P3HT:PCBM:Q-switch 1 = 1:1:1, and (c) P3HT:PCBM:Ir-125:Q-switch 1 = 1:1:0.5:0.5.

sities, we further performed the spectrally resolved EQE measurements; Fig. 3 displays the EQE results of various devices. The highest EQE of the device containing Ir-125 was  $\sim 8000\%$  [Fig. 3(a)]; the result was consistent with our previous report.<sup>10</sup> In contrast, the highest EQE value of the device prepared with Q-switch 1 was only  $\sim 840\%$  at a bias of  $-5.0 \text{ V}$  [Fig. 3(b)]. The reason for the lower efficiency could be understood from the energy level diagram of the device [the inset to Fig. 2(a)]. Unlike Ir-125, Q-switch 1 molecules can trap electrons and holes simultaneously in the P3HT:PCBM blend. Because the photoconduction gain arises from unbalanced carrier transport,<sup>17</sup> trapping of both types of charges improved the balance of charge transport,

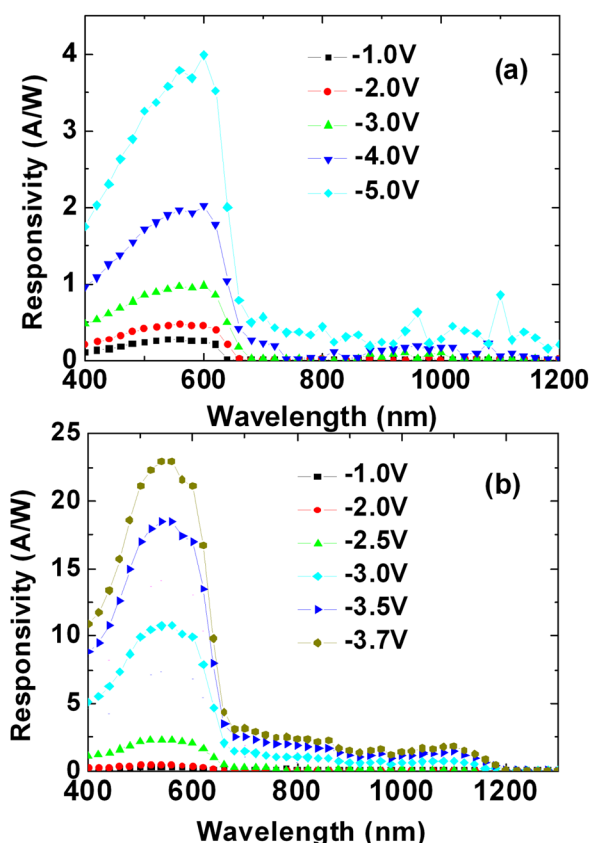


FIG. 4. (Color online) Spectrally resolved responsivities ( $R$ ) of the dye-doped devices, recorded under various bias conditions. Dopant weight ratios in the active layers: (a) P3HT:PCBM:Q-switch 1=1:1:1 and (b) P3HT:PCBM:Ir-125:Q-switch 1=1:1:0.5:0.5.

thereby decreasing the values of EQE. More interestingly, after the addition of both Ir-125 and Q-switch 1 molecules, the efficiencies was dramatically increased [Fig. 3(c)]. In the visible region, the highest EQE was approximately 5500% ( $\lambda = 510$  nm). Further, the spectral response region was extended to 1200 nm. Besides, EQEs higher than 100% in the NIR region could be also achieved (up to 200%).

The improved photoresponse of the codoped device was probably due to the increased trapping probability of electrons, thereby altering the charge balance. As shown in the energy level diagram [the inset to Fig. 2(a)], Ir-125 molecules prefer to trap electrons solely. Therefore, the addition of Ir-125 into the photoactive layer overall increased the lifetime of the electrons in the device, thereby increasing the current gain. As a result, although the highest EQE ( $\sim 5500\%$ ) was still lower than that of the device incorporating a single kind of NIR molecules, Ir-125 [Fig. 3(a)], which was probably due to the lower concentration of Ir-125 molecules, the codoped device exhibited pronounced PM effect over a broad wavelength range covering from 400 to 1200 nm.

From Fig. 3, we could see that the EQE values in the NIR region were much less than those in the visible region while NIR dopants exhibited comparable absorption with P3HT and PCBM molecules. We suspected that two possible reasons maybe responsible for this phenomenon. First, the anode structure consisting of ITO and PEDOT:PSS layers had considerable absorption in the NIR region, which may block part of the incident light into the active layer. Moreover, after the NIR photons were absorbed by the dopants,

the energy was much easier to be dissipated as heat (or non-radiative decay) rather than free charges. Therefore, charges are much more difficult to be collected, leading to lower values of EQEs. More detailed studies are ongoing.

Figure 4 displays the spectrally resolved responsivities ( $R$ , in units of A/W), defined as the ratio of photocurrent to the input light intensity,<sup>10,18</sup> for the devices prepared with NIR dopants. For the Q-switch 1-doped device, the highest responsivity was 4.0 A/W in the visible region under a reverse bias of  $-5.0$  V [Fig. 4(a)]. Nevertheless, as shown in Fig. 4(b), the responsivities significantly increased upon the addition of Ir-125 molecules. The highest responsivity was 23.0 A/W at a wavelength of 560 nm under a reverse bias of  $-3.7$  V. Further, the device responsivity remained high in the NIR region. For example, the  $R$  values were 3.2 and 1.8 A/W at the wavelength of 700 and 1100 nm, respectively.

In conclusion, we have developed highly sensitive OPDs with spectral response extending from the ultraviolet to the near-infrared region; the spectral response range should be one of the widest ones among the OPDs exhibiting photoconductive gains. After doping two organic NIR dyes into the active layer, we have achieved a high EQE ( $\sim 5500\%$ ) and a high responsivity (23.0 A/W) under a low reverse bias. Meanwhile, substantially improved EQEs higher than 200% at the NIR region have been demonstrated. This approach reported here allows the ready preparation of polymer photodetectors exhibiting broad spectral responses and high quantum efficiencies simultaneously.

We thank the National Science Council of Taiwan (NSC 99-2221-E-009-181 and NSC 100-2221-E-009-082) and the Ministry of Education of Taiwan (through the ATU program) for financial support.

- <sup>1</sup>T. Rauch, M. Bobber, S. F. Tedde, J. Furst, M. V. Kovalenko, G. N. Hesser, U. Lemmer, W. Heiss, and O. Hayden, *Nat. Photonics* **3**, 332 (2009).
- <sup>2</sup>Y. Yao, Y. Y. Liang, V. Shrotriya, S. Q. Xiao, L. P. Yu, and Y. Yang, *Adv. Mater.* **19**, 3979 (2007).
- <sup>3</sup>G. J. Matt, T. Fromherz, M. Bednorz, S. Zamiri, G. Goncalves, C. Lungenschmied, D. Meissner, H. Sitter, N. S. Sariciftci, C. J. Brabec, and G. Bauer, *Adv. Mater.* **22**, 647 (2010).
- <sup>4</sup>T. Someya, Y. Kato, S. Iba, Y. Noguchi, T. Sekitani, H. Kawaguchi, and T. Sakurai, *IEEE Trans. Electron. Devices* **52**, 2502 (2005).
- <sup>5</sup>X. Xu, M. Davanco, X. F. Qi, and S. R. Forrest, *Org. Electron.* **9**, 1122 (2008).
- <sup>6</sup>X. Gong, M. H. Tong, Y. J. Xia, W. Z. Cai, J. S. Moon, Y. Cao, G. Yu, C. L. Shieh, B. Nilsson, and A. J. Heeger, *Science* **325**, 1665 (2009).
- <sup>7</sup>M. S. Arnold, J. D. Zimmerman, C. K. Renshaw, X. Xu, R. R. Lunt, C. M. Austin, and S. R. Forrest, *Nano Lett.* **9**, 3354 (2009).
- <sup>8</sup>M. Hiramoto, T. Imahigashi, and M. Yokoyama, *Appl. Phys. Lett.* **64**, 187 (1994).
- <sup>9</sup>H. Y. Chen, M. K. F. Lo, G. W. Yang, H. G. Monbouquette, and Y. Yang, *Nat. Nanotechnol.* **3**, 543 (2008).
- <sup>10</sup>F. C. Chen, S. C. Chien, and G. L. Cious, *Appl. Phys. Lett.* **97**, 103301 (2010).
- <sup>11</sup>S. H. Wu, W. L. Li, B. Chu, Z. S. Su, F. Zhang, and C. S. Lee, *Appl. Phys. Lett.* **99**, 023305 (2011).
- <sup>12</sup>W. T. Hammond and J. Xue, *Appl. Phys. Lett.* **97**, 073302 (2010).
- <sup>13</sup>J. Reynaert, V. I. Arkhipov, P. Heremans, and J. Poortmans, *Adv. Funct. Mater.* **16**, 784 (2006).
- <sup>14</sup>I. H. Campbell and B. K. Crone, *J. Appl. Phys.* **101**, 024502 (2007).
- <sup>15</sup>J. Huang and Y. Yang, *Appl. Phys. Lett.* **91**, 203505 (2007).
- <sup>16</sup>V. Shrotriya, G. Li, Y. Yao, T. Moriarty, K. Emery, and Y. Yang, *Adv. Funct. Mater.* **16**, 2016 (2006).
- <sup>17</sup>G. Konstantatos and E. H. Sargent, *Nat. Nanotechnol.* **3**, 543 (2008).
- <sup>18</sup>J. Gao and F. A. Hegmann, *Appl. Phys. Lett.* **93**, 223306 (2008).